ELSEVIER

1 July 2000

Optics Communications 181 (2000) 183–190

OPTICS COMMUNICATIONS

www.elsevier.com/locate/optcom

Nonlinear formation of dynamic holograms and multiwave mixing in resonant media

A.S. Rubanov, A.L. Tolstik *, S.M. Karpuk, O. Ormachea

Department of Laser Physics and Spectroscopy, Belarusian State University, 4 F.Skaryna Ave., Minsk 220050, Belarus

Received 27 January 2000; received in revised form 18 April 2000; accepted 3 May 2000

Abstract

The schemes of light beam transformations by volume dynamic holograms in resonant media revealing the fifth- or higher-order nonlinearities have been theoretically analyzed. *N*-wave mixing has been realized by changing of the propagation direction or frequency of the read-out wave in the solution of Rhodamine 6*G* and polymethine 3274*U* dyes. It has been demonstrated that the experimental results are in good agreement with the theoretical data obtained for a three-level medium model with due regard to absorption from the excited singlet level. © 2000 Published by Elsevier Science B.V.

PACS: 42.65.Hw
Keywords: Dynamic holograms; Multiwave mixing; Resonant media; Higher-order nonlinearities

1. Introduction

One of the most promising elements of optical data processing systems are the dynamic diffraction (holographic) structures making it possible to control information light fields. So far practically all the investigations into the information capacity of diffraction methods have been concerned only with the linearity approximation for holographic recording of the wave front. However, a number of materials (semiconductor glasses, dyes, atomic media) are characterized by a high level of the fifth- or higher-order nonlinearity leading to distortion of the holographic-grating groove profile. Such a nonlinear recording of holograms has been traditionally considered as a negative factor resulting in the emergence of noise components in the diffracted radiation [1]. At the same time, high priority of the investigations associated with the development of control elements for laser fluxes stimulates researchers to analyze new means of information processing on the basis of nonlinear holographic elements (spatial filtration, associative memory, visualization of complex phase portraits [2–4]). Due to the effect of absorption saturation, higher-order nonlinearities in resonant media manifest themselves together with the cubic nonlinearity permitting realization of *N*-wave mixing. In this case, new components emerge as a result of expanding the medium susceptibility into a series of dynamic grating components and provide a means for the Bragg reading-beam diffraction of the second and higher orders.

Dynamic gratings are recorded by signal E_S and reference E_1 waves having the same frequency ω. Condition of the Mth-order Bragg diffraction ($M =$

* Corresponding author. E-mail: tolstik@phys.bsu.unibel.by

0030-4018/00/$ - see front matter © 2000 Published by Elsevier Science B.V.
PII: S0030-4018(00)00743-4

$N/2-1$) is satisfied through an increase of the reading angle or through a change in the reconstructing-wave frequency. The experiments performed for measurement of the higher-order susceptibilities with the use of gases [5,6], semiconductor glasses [7,8], dyes [8,9] as nonlinear media were based on recording and reconstruction of dynamic gratings at the same frequency. Fulfillment of the Bragg condition was achieved by changing an incidence angle of the reconstructing beam. In the second case the reconstructing wave E_2 had a frequency $M\omega$ and was counter-propagating relative to the reference one. This resulted in phase conjugation with simultaneous conversion of the radiation frequencies [10–13]. Both parametric scattering schemes have been illustrated in Fig. 1 for the case of six-wave mixing ($N=6$, $M=N/2-1=2$).

In this report we present theoretical and experimental analysis of the schemes for multiwave mixing realized in media with saturable (resonance, thermal) nonlinearity in conditions revealing nonlinearity of the fifth- and higher-orders. Let us consider both cases of dynamic hologram reconstruction (at frequencies ω and $M\omega$). A dynamic hologram was formed by signal $E_S = A_S\exp[\mathrm{i}(\boldsymbol{k}_S(\omega)\boldsymbol{r} - \omega t + \varphi_S)]$ and reference $E_1 = A_1\exp[\mathrm{i}(\boldsymbol{k}_1(\omega)\boldsymbol{r} - \omega t + \varphi_1)]$ waves; it was reconstructed by the wave $E_2 = A_2\exp[\mathrm{i}(\boldsymbol{k}_2(\omega)\boldsymbol{r} - \omega t + \varphi_2)]$ or $E_2 = A_2\exp[\mathrm{i}(\boldsymbol{k}_2(M\omega)\boldsymbol{r} - M\omega t + \varphi_2)]$ counter-propagating relative to the reference one. Under the conditions of nonlinear formation of a dynamic grating the induced nonlinear polarization $P = \chi^{(N-1)}(E_1E_S^*)^M E_2$ was responsible for generation of the wave E_D. The wave E_D direction is determined by the condition of phase synchronism $\boldsymbol{k}_D = M\boldsymbol{k}_1 - M\boldsymbol{k}_S + \boldsymbol{k}_2$. And in case of the hologram reconstruction at the frequency $M\omega$ with opposite propagation directions of the plane reference and reconstructing waves $\boldsymbol{k}_2(M\omega) + M\boldsymbol{k}_1(\omega) = 0$, the induced wave E_D propagates counter to the signal one E_S.

2. Theoretical model of degenerate multiwave mixing

A theoretical study of the efficiency of N-wave mixing is carried out for resonant media simulated with three-level schemes taking into account transitions in the ground singlet $S_0 - S_1$ as well as in the excited singlet $S_1 - S_2$ channels. Triplet states of the molecules may be disregarded in our work since the consideration is being given to analysis of short time interactions ($\sim 10^{-8}$ s) during which the triplet levels remain practically nonpopulated (the intersystem crossing rates are slow on the time scale of the experiments). Considering that the intensity of interacting waves is, as a rule, much lower than the absorption saturation intensity in the excited channel, during recording of nonlinear susceptibility one should take into account the saturated absorption in the ground singlet channel and induced absorption from the excited level. Such a model may be used to

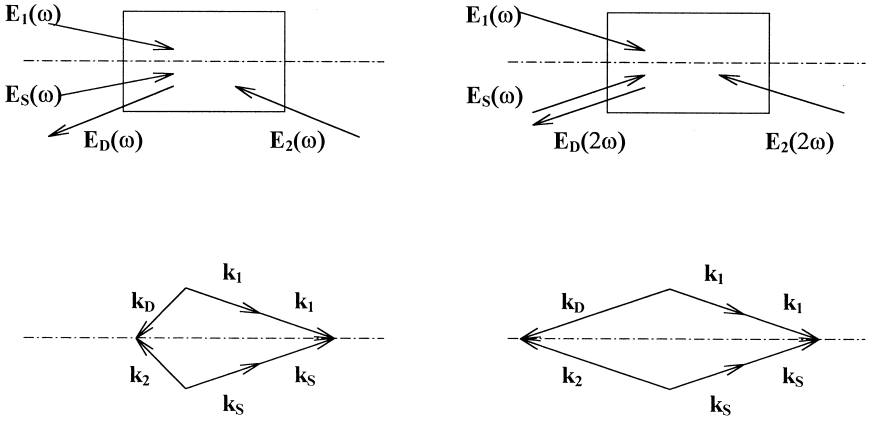

Fig. 1. Mixing geometry and phase-matching diagrams for the case of six-wave mixing.

describe the energy states of numerous complex compounds (liquid and solid dye solutions, colored crystals, and vapors of complex organic compounds).

With the aim of calculating the nonlinear properties of the resonant medium, we use a standard solution of kinetic equations for the level populations and the Kramers–Kronig relations relating the real and imaginary parts of the complex refractive index $\hat{n} = n + \mathrm{i}\varkappa$ (dispersion relations, e.g. Refs. [14,15]). In this case the complex refractive index determined by resonance transitions in the ground singlet channel $S_0 - S_1$ and by absorption from the excited level S_1 may be given as [15,16]:

$$\hat{n} = n + \mathrm{i}\varkappa = \frac{\hbar c}{2\upsilon}\left(N_1\hat{\Theta}_{12} - N_2\hat{\Theta}_{21} + N_2\hat{\Theta}_{23}\right), \quad (1)$$

where N_1 and N_2 are populations of the energy levels S_0 and S_1; $\upsilon = c/n_0$ is the light velocity of the medium; n_0 is a nonresonant component of the refractive index. The coefficients $\hat{\Theta}_{lj}(\omega) = \Theta_{lj}(\omega) + \mathrm{i}B_{lj}(\omega)$ represent a complex function describing the spectral properties of the resonant transition $l - j$. And $\Theta_{lj}(\omega)$ is related to Einstein coefficient for stimulated transitions $B_{lj}(\omega)$ through the dispersion relations: $\Theta_{lj}(\omega) = \frac{1}{\pi}\int_{-\infty}^{\infty} B_{lj}(\omega')/(\omega' - \omega)\mathrm{d}\omega'$ [15].

A change in the refractive index due to the medium heating is determined by thermalization of the absorbed energy both in the ground singlet $S_0 - S_1$ and in the excited singlet $S_1 - S_2$ channels. Thermally induced changes of the refractive index in conditions of adiabatic heating may be introduced in the following way [16]:

$$\Delta n_t = (\mathrm{d}n/\mathrm{d}T)\Delta T = 2\omega\left(\varkappa_{12}(1-\mu_{21}) + \varkappa_{23}(1-\mu_{32})\right)(\mathrm{d}n/\mathrm{d}T)I\tau/cC_p, \quad (2)$$

where $\varkappa_{12}$, $\varkappa_{23}$ are the extinction coefficients determining absorption in the ground 1–2 ($S_0 - S_1$) and excited 2–3 ($S_1 - S_2$) channels ($\varkappa = \varkappa_{12} + \varkappa_{23}$); μ_{lj} is the luminescence quantum yield in the $l - j$ channel; $\mathrm{d}n/\mathrm{d}T$ is the thermo-optical coefficient; C_p is the unit-volume heat capacity; I is light field intensity in the medium. τ is the characteristic duration of the interaction, and τ is the light pulse duration for excitations when heat withdrawal processes could be neglected. This approach allows for molecular transitions to the excited states and for the Stokes shift of absorption and emission bands associated with complex organic molecules [16].

Using the stationary solution of a system of kinetic equations for the energy level populations N_l in a three-level medium model with regard to the expressions (1), (2), the medium susceptibility may be represented as

$$\chi(\omega) = \frac{n_0\varkappa_0}{2\pi}\left(\frac{\hat{\Theta}_{12}}{B_{12}} - \frac{\hat{\alpha}I - b_t I^2}{1 + JI}\right), \quad (3)$$

where

$$\hat{\alpha} = a + \mathrm{i}\alpha = \left(\hat{\Theta}_{12} + \hat{\Theta}_{21} - \hat{\Theta}_{23}\right)/\upsilon P_{21} - \sigma \times (1 - \mu_{21}),$$

$$b_t = \sigma B_{23}(1 - \mu_{32})/\upsilon P_{21},$$

$$J = (B_{12} + B_{21})/\upsilon P_{21}.$$

Here $\varkappa_0$ is the linear extinction coefficient; P_{21} is the summary probability of spontaneous and nonradiative transitions between the levels S_1 and S_0; $\sigma = 2\omega(\mathrm{d}n/\mathrm{d}T)\tau/cC_p$.

Under the conditions of the Mth-order Bragg diffraction, coupled equations describing the formation of a diffracted wave are as follows:

$$\frac{\partial E_1}{\partial r} = \frac{\mathrm{i}2\pi\omega}{cn_0}\left[\chi_{0,0}E_1 + \chi_{1,1}E_2 + \chi_{1,0}E_S + \chi_{1-M,1}E_D\right],$$

$$\frac{\partial E_2}{\partial r} = -\frac{\mathrm{i}2\pi\omega}{cn_0}\left[\chi_{0,0}E_2 + \chi_{-1,-1}E_1 + \chi_{0,-1}E_S + \chi_{-M,0}E_D\right],$$

$$\frac{\partial E_S}{\partial r} = \frac{\mathrm{i}2\pi\omega}{cn_0}\left[\chi_{0,0}E_S + \chi_{-M,1}E_D + \chi_{-1,0}E_1 + \chi_{0,1}E_2\right],$$

$$\frac{\partial E_D}{\partial r} = -\frac{\mathrm{i}2\pi\omega}{cn_0}\left[\chi_{0,0}E_D + \chi_{M,-1}E_S + \chi_{M-1,-1}E_1 + \chi_{M,0}E_2\right], \quad (4)$$

where

$$\chi_{m,n} = \frac{1}{(2\pi)^2}\int_{-\pi}^{\pi}\int_{-\pi}^{\pi}\chi(\zeta_x,\zeta_y) \times \exp\left[-\mathrm{i}(m\zeta_x + n\zeta_y)\right]\mathrm{d}\zeta_x\mathrm{d}\zeta_y,$$

$$\zeta_x = (\boldsymbol{k}_1 - \boldsymbol{k}_S)\boldsymbol{r}, \quad \zeta_y = (\boldsymbol{k}_S - \boldsymbol{k}_2)\boldsymbol{r}.$$

The term with $\chi_{0,0}$ takes into account modulation of both the absorption coefficient and refractive index through a medium bleaching in the field of interacting waves. $\chi_{\pm 1,\pm 1}$, $\chi_{0,\pm 1}$, $\chi_{\pm 1,0}$ describe the self-diffraction reference, signal and reconstructing waves. Other Fourier-expansion components define formation of the wave E_D through diffraction from the second and higher-order spatial components of dynamic gratings.

A system of equations (4) is considerably reduced in case when the reconstructing wave E_2 is not interfering with reference and signal waves, and analysis of the interaction efficiency may be limited to diffraction of the wave E_2 from the grating formed by the waves E_1 and E_S

$$\frac{\partial E_{1,S}}{\partial r} = \frac{\mathrm{i}2\pi\omega}{cn_0}\left[\chi_0 E_{1,S} + \chi_{\pm 1}E_{S,1}\right],$$

$$\frac{\partial E_{2,D}}{\partial r} = -\frac{\mathrm{i}2\pi\omega}{cn_0}\left[\chi_0 E_{2,D} + \chi_{\mp M}E_{D,2}\right], \qquad (5)$$

where

$$\chi_m = \frac{1}{2\pi}\int_{-\pi}^{\pi}\chi(\zeta)\exp\left[-\mathrm{i}m\zeta\right]\mathrm{d}\zeta,$$

$$\zeta = (\boldsymbol{k}_1 - \boldsymbol{k}_S)\boldsymbol{r}.$$

With the use of Eq. (3) and expression for the intensity of interacting waves in the nonlinear medium, $I = I_1 + I_2 + I_S + I_D + 2\sqrt{I_1 I_S}\cos\zeta$, the components of expansion for nonlinear susceptibility χ_m in a three-level resonant medium model may be written in the explicit form

$$\chi_0 = \frac{n_0\varkappa_0}{2\pi}\left(\frac{\hat{\Theta}_{12}}{B_{12}} + \frac{b_t}{J}I_\Sigma + \left(\hat{\alpha}/J + b_t/J^2\right)\frac{1-A_0}{A_0}\right), \qquad (6)$$

$$\chi_{\pm 1} = \frac{n_0\varkappa_0}{2\pi}\left(\frac{b_t}{J}\sqrt{I_1 I_S} - \left(\hat{\alpha}/J + b_t/J^2\right) \times \frac{2J\sqrt{I_1 I_S}}{A_0(1 + JI_\Sigma + A_0)}\right)\exp\left[\pm\mathrm{i}(\varphi_1 - \varphi_S)\right], \qquad (7)$$

$$\chi_{\pm M} = \frac{n_0\varkappa_0}{2\pi}\left(\hat{\alpha}/J + b_t/J^2\right)\frac{\left(-2J\sqrt{I_1 I_S}\right)^M}{A_0(1 + JI_\Sigma + A_0)^M} \times \exp\left[\pm\mathrm{i}M(\varphi_1 - \varphi_S)\right], \qquad (8)$$

where $A_0 = \left((1 + JI_\Sigma)^2 - 4J^2 I_1 I_S\right)^{1/2}$, $I_\Sigma = I_1 + I_2 + I_S + I_D$ is the total intensity of interacting waves.

As follows from Eqs. (5) and (8) for plane reference and reconstructing waves ($\varphi_2 + M\varphi_1 = \text{const}$), the phase of a diffracted wave is a multiple to the phase of the signal one ($\varphi_D = -M\varphi_S$). In this way the light beams diffracted from different spatial components of the dynamic grating are distinguished by the propagation direction as well as spatial structure of the wave front. Using the Mth-order Bragg diffraction makes it possible to enhance the wave front phase distortions.

3. Theoretical model of nondegenerate *N*-wave mixing

This section presents a case of the frequency-nondegenerate multiwave mixing, when a dynamic hologram is recorded at a frequency ω and the reconstructing wave has a frequency $M\omega$. Such a situation for resonant media results in practical transparency of the medium at a frequency $M\omega$ provided it absorbs radiation at a frequency ω. In this case, the formation of the diffracted wave is determined by diffraction of the reconstructing wave E_2 from a thermal dynamic grating formed by the signal and reference waves. For a three-level medium model incorporating induced absorption from the excited level, the susceptibility conditioned by thermal nonlinearity Δn_t (2) at a frequency $M\omega$ may be written in the form similar to the Eq. (3)

$$\chi(M\omega) = \frac{n_0\varkappa_0}{2\pi}\left(\frac{a_t I + b_t I^2}{1 + JI}\right), \qquad (9)$$

where $a_t = \sigma(1-\mu_{21})$. The remaining members are interpreted in explanation for the expression (3).

A system of equations describing multiwave mixing for nonlinear polarization $P = \chi^{(N-1)}(E_1 E_S^*)^M E_2$ is of the following form:

$$\frac{\partial E_{1,S}}{\partial r} = \frac{\mathrm{i}2\pi\omega}{cn_0}\left[\chi_0(\omega)E_{1,S} + \chi_{\pm 1}(\omega)E_{S,1}\right],$$

$$\frac{\partial E_{2,D}}{\partial r} = -\frac{\mathrm{i}2\pi M\omega}{cn_0}\left[\chi_0(M\omega)E_{2,D} + \chi_{\mp M}(M\omega)E_{D,2}\right]. \quad (10)$$

Taking into consideration a particular form of nonlinear susceptibility (3), (9), a system of equations (10) for the case of six-wave mixing ($M=2$) may be transformed as follows:

$$\frac{\partial E_{1,S}}{\partial r} = \frac{\mathrm{i}k_0}{2} f_{1,S} E_{1,S},$$

$$\frac{\partial E_{2,D}}{\partial r} = -\mathrm{i}k_0\left(\psi E_{2,D} + \phi E_{D,2} \times \exp\left[\mp \mathrm{i}2(\varphi_1 - \varphi_S)\right]\right), \quad (11)$$

where $k_0 = 2\omega\varkappa_0/c$ is the initial absorption coefficient,

$$f_{1,S} = \frac{\hat{\Theta}_{12}}{B_{12}} + \frac{b_t}{J}(I_{1,S} + 2I_{S,1}) - \left(\hat{\alpha}/J + b_t/J^2\right) \times \left(1 - \frac{1}{A} + \frac{2JI_{S,1}}{A(1+J(I_1+I_S)+A)}\right),$$

$$\psi = \frac{b_t}{J}(I_1 + I_S) + \left(a_t/J - b_t/J^2\right)(1 - 1/A),$$

$$\phi = \left(a_t/J - b_t/J^2\right)\left(\frac{1}{A} - \frac{2(1+J(I_1+I_S))}{A(1+J(I_1+I_S)+A)}\right),$$

and $A = \left(1 + 2J(I_1+I_S) + J^2(I_1 - I_S)^2\right)^{1/2}$.

From (11) it follows that for the plane waves E_1 and E_2 the phase of a diffracted wave is $\varphi_D = -2\varphi_S$. Considering that the signal and diffracted waves are counter-propagating (Fig. 1), this is an indication that the waves E_S and E_D have coincident surfaces of the wave front (phase of the diffracted wave follows the frequency changes).

The factor $(a_t - b_t/J)$ entering into the expression for ϕ describes the dependence of the diffracted-wave formation efficiency on the spectral characteristics of a medium:

$$a_t - b_t/J = \sigma\left[(1-\mu_{21}) - k_r(1-\mu_{32})/k_0\right]. \quad (12)$$

Here, $k_r = k_0 B_{23}/(B_{12}+B_{21})$ is the coefficient of residual absorption, k_0 is the initial absorption coefficient. The above formulae enable one to determine the conditions of the efficient light-field conversion. Specifically, from (12) it is obvious that on condition the equality $k_r(1-\mu_{32}) = k_0(1-\mu_{21})$ is satisfied, diffraction is absent since in this case the medium is a linearly absorbing one: $\chi(2\omega) \sim I$, $\chi_{\pm 2}(2\omega) = 0$.

It should be noted that the above equations have been derived for the writing conditions of transmission dynamic holograms (following propagation of signal and reference waves). When a hologram is written by counter-propagating beams (in case of reflection holograms), multiwave mixing is described by similar equations with a proper change of sign. A comparative theoretical analysis of nondegenerate six-wave mixing from transmission and reflection dynamic holograms is given in [12] together with a more general spectroscopic model of the resonant medium including saturation of the absorption from the ground singlet and excited singlet or triplet states of molecules.

4. Experimental realization of multiwave mixing

Both methods of multiwave mixing have been realized on the basis of Nd:YAG laser using the Rhodamine 6*G* and polymethine 3274*U* dyes. In case of the frequency-degenerate multiwave mixing we used the second harmonic of Nd:YAG laser (wavelength $\lambda = 0.532$ μm; pulse energy $W \simeq 30$ mJ; duration $\tau \simeq 30$ ns; repetition rate of 1 Hz and divergence $\leqslant 2$ mrad) corresponding to the absorption band maximum of the Rhodamine 6*G* dye solution in ethanol. Diffraction of different orders from a volume holographic grating has been realized at different propagation directions of a reconstructing wave, conforming to the condition of Bragg diffraction from different spatial components of the grating.

We used the experimental setup shown in Fig. 2. Fundamental radiation of the laser was reflected by the spectral splitter (2), whereas the second harmonic

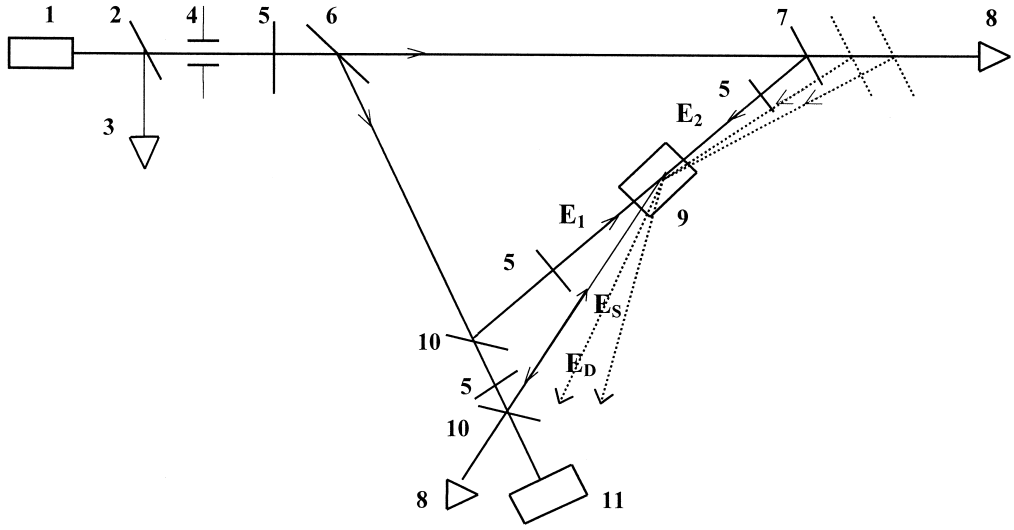

Fig. 2. Experimental setup: (1) laser; (2) spectral splitter; (3) IR radiation absorber; (4) aperture; (5) optical filters; (6,7,10) mirrors; (8) recording system; (9) cell with dye solution; (11) meter for measuring the laser radiation energy. Reflection coefficients of mirrors are $R_6 = R_{10} = 0.5$, $R_7 = 0.99$.

radiation was transmitted. An aperture 3 mm in diameter selected the spatially homogeneous part of the radiation. The mirrors (6,10) formed the signal and reference waves. A mirror (7) directed the reconstructing wave opposite to the reference one. The mirror (7) was movable to permit variation of the read-out angle. Filters (5) enabled one to alter the intensity of the interacting waves. The intensity of recording waves was monitored with a laser energy meter (11). The energy efficiency of the radiation conversion (i.e. the intensity ratio of the diffracted and reconstructing beams) was determined by a recording system (8).

The diffraction efficiency of conversion $\xi = I_D/I_2$ as a function of the angle β between reconstructing and reference waves is given in Fig. 3. The angle between the recording waves was $\alpha \simeq 30$ mrad. For the counter-propagating reconstructing wave ($\beta = 0$) a classical case of phase conjugation upon four-wave mixing has been effected. The second maximum in the dependence of diffraction efficiency on the reading angle was observed with $\beta \approx \alpha/2$, and conformed to the phase synchronism condition $\boldsymbol{k}_D = 2\boldsymbol{k}_1 - 2\boldsymbol{k}_S + \boldsymbol{k}_2$ (Fig. 1). As previously stated, it is attributed to the fifth-order nonlinearity ($P \sim (E_1 E_S^*)^2 E_2$). The third maximum in the region of $\beta \approx \alpha$ conforms to the condition of phase synchronism $\boldsymbol{k}_D = 3\boldsymbol{k}_1 - 3\boldsymbol{k}_S + \boldsymbol{k}_2$. In this case the eight-wave mixing is registered at the seventh-order nonlinearity ($P \sim (E_1 E_S^*)^3 E_2$).

It should be noted that differing propagation directions and wave phases of the diffracted beams in the above cases provide a means for simultaneous realization of various wavefront transformations.

In case of the frequency-nondegenerate six-wave mixing a dynamic hologram was recorded at the

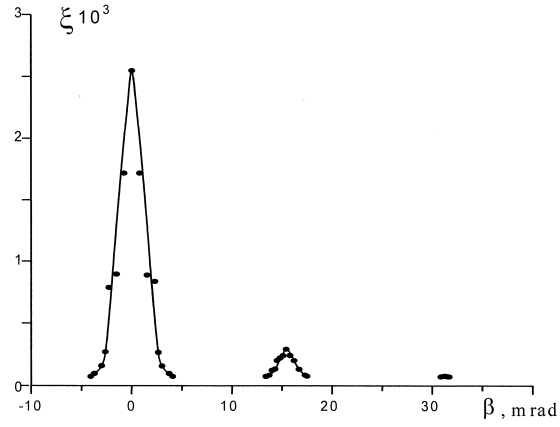

Fig. 3. Diffraction efficiency $\xi = I_D/I_2$ as a function of the incidence angle of reconstructing beam for Rhodamine 6G dye at $k_0 L = 1.2$ and $I_1 = 2I_S = 0.6$ MWcm^{-2}, and solid lines are just a guide for the eye.

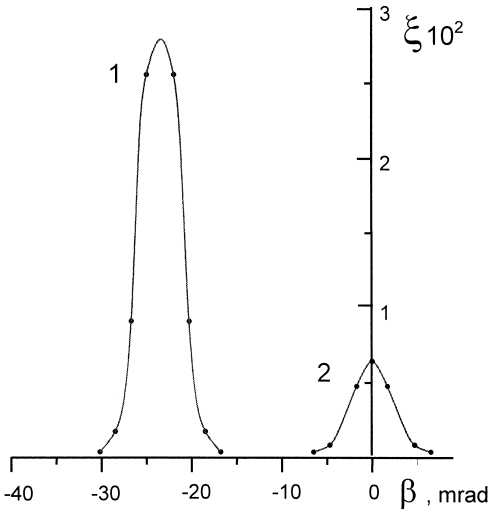

Fig. 4. Diffraction efficiency ξ as a function of the incidence angle of reconstructing beam for polymethine dye 3274*U* at $k_0 L = 3$ and $I_1 = I_S = 8$ MWcm^{-2}. An $\times 10$ magnification was used for the diffraction efficiency values associated with the curve 2, and solid lines are just a guide for the eye.

fundamental wavelength of Nd:YAG laser ($\lambda =$ 1.064 μm; lasing energy $W \simeq$ 200 mJ; pulse width $\tau \simeq$ 10 ns), corresponding to the absorption band maximum of the solution of polymethine dye 3274*U* in isobutyl alcohol. Bleaching intensity was ~ 13 MWcm^{-2}, lifetime of molecules in the excited state ~ 10 ps [17]. Experimental setup was the same, as in the previous case (Fig. 2), except for a semitransparent mirror (6) replaced by the spectral splitter (2). This spectral splitter reflected radiation at the fundamental lasing frequency ($\lambda = 1.064$ μm) to be used for the recording of dynamic holograms. The transmitted radiation at the second harmonic frequency ($\lambda = 0.532$ μm) was not actually absorbed by the dye solution and could be efficiently used for hologram reconstruction.

Fig. 4 shows the diffraction efficiency of conversion $\xi = I_D/I_2$ as a function of the angle β between reconstructing and reference waves. The angle between the recording waves was $\alpha \simeq 90$ mrad. The first maximum ($\beta \simeq -23$ mrad) is due to linear recording of dynamic holograms with the polarization $P \sim E_1 E_2 E_S^*$ responsible for generation of the wave E_D at a double frequency 2ω. The value of $|\beta| \simeq 23$ mrad $\approx \alpha/4$ is associated with phase synchronism $\boldsymbol{k}_D = \boldsymbol{k}_1 - \boldsymbol{k}_S + \boldsymbol{k}_2$ leading to an angle between the diffracted and reconstructing waves that is small compared to the angle between the hologram recording beams. As this takes place, the diffracted wave retains the phase of the signal one but the frequency is growing in line with smoothing of the wave-front spatial structure. Frequency conversion of simple images is possible with the use of a practically plane signal wave. It is essential that the condition of phase synchronism for the variant of nondegenerate four-wave mixing under consideration may be met only at the preassigned direction of a signal wave [18]. The conversion of IR-image to the visible in the process of recording thermal dynamic holograms has been experimentally realized in [19].

The presence of the second maximum in $\xi(\beta)$ for $\beta = 0$ (Fig. 4) is due to the quadratic recording method of dynamic holograms with the diffraction determined by the second components in the medium susceptibility expansion into harmonics of the dynamic grating and the induced nonlinear polarization $P \sim (E_1 E_S^*)^2 E_2$. In this case ($2\boldsymbol{k}_1 + \boldsymbol{k}_2 = 0$) the induced wave E_D is counter-propagating to the signal one E_S ($\boldsymbol{k}_D = -2\boldsymbol{k}_S$) and has a double conjugate phase $\varphi_D = -2\varphi_S$, i.e. these waves possess the features of phase-conjugate waves. A comparative analysis of the diffraction efficiency of linearly and quadratically formed dynamic holograms is presented in [20]. The ratio of the diffraction efficiencies observed in our experiment is in good agreement with the theoretical results. The dependence of the diffraction efficiency $\xi = I_D/I_2$ of a quadratically

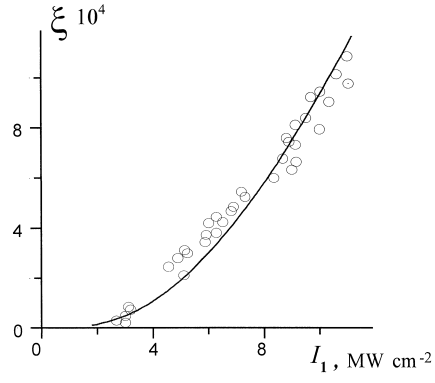

Fig. 5. Experimental (circles) and calculated (solid line) dependences of the diffraction efficiency ξ on the intensity of the hologram-recording waves $I_1 = I_S$ for $k_0 L = 3$, $\beta = 0$.

recorded dynamic hologram on the intensity of the reference wave I_1 (in our experiments $I_1 = I_S$) is plotted in Fig. 5. The conversion efficiency $\xi \approx 10^{-3}$ was three orders of magnitude higher than the efficiency of a dynamic hologram formation in polymers by resonant two-photon absorption [3].

The solid line in Fig. 5 gives the calculated function of the diffraction efficiency. The calculations were performed using the formalism (11) for a three-level medium model, the applicability of which to the description of nonlinear processes in the solution of polymethine dye 3274*U* has been noted in [21]. Parameters of the medium and radiation correspond to the experimental conditions ($n_0 = 1.36$, $(\mathrm{d}n/\mathrm{d}T)C_p^{-1} = -1.5 \times 10^{-4}$ $\mathrm{J}^{-1}\mathrm{cm}^3$, $B_{23}/B_{12} = 0.43$). The quantum efficiency of luminescence in the ground and excited channels is close to zero $\mu_{21} \approx 0.003$, $\mu_{32} \approx 0.0001$ [17,21,22]. The diffraction efficiency versus intensity of the waves forming a hologram at the entry to the nonlinear medium is plotted in Fig. 5 with a normalization factor $1/3$, considering that solution of the coupled equations gives the diffraction efficiency at the end of a pulse. And the experimental results give the efficiency averaged over the whole pulse [23]. A good quantitative agreement is observed between the experimental and theoretical data. This correlation has made it possible to estimate the value of the fifth-order nonlinear optical susceptibility $\chi^{(5)}$ as $\sim 4 \times 10^{-16}$ units esu [24].

5. Conclusion

In conclusion it should be noted that the potentialities of the diffraction methods used for optical data processing and determination of the medium nonlinear optical characteristics may be widened considerably. This is demonstrated by the presented schemes for transformation of light fields with the nonlinearly formed dynamic holograms. In the process of multiwave mixing the diffracted beams are distinguished not only by the propagation direction, but also by the wave phase, providing for simultaneous realization of various wavefront conversions. Combination of the wavefront conjugation and radiation frequency conversion may be used for visualization of IR images with the complex spatial structure, distortion compensation for radiation propagating in the phase-inhomogeneous media.

References

[1] R.J. Collier, C.B. Burckhardt, L.H. Lin, Optical Holography, Academic Press, 1971.
[2] P.B. Polyanskii, Opt. Spektrosk. 65 (1988) 435, in Russian; Opt. Spectrosc. 65 (1988) 258.
[3] F. Charra, J.-M. Nunzi, J. Opt. Soc. Am. B 8 (1991) 570.
[4] S.M. Karpuk, A.S. Rubanov, A.L. Tolstik, A.V. Chaley, Proc. SPIE 2771 (1995) 149.
[5] R.K. Raj, Q.F. Gao, D. Bloch, M. Ducloy, Opt. Commun. 51 (1984) 117.
[6] J.W.R. Tabosa, C.L. Cesar, M. Ducloy, J.R. Rios Leite, Opt. Commun. 67 (1988) 240.
[7] A. Blouin, P. Galarneau, M.-M. Denariez-Roberge, Opt. Commun. 72 (1989) 249.
[8] A. Blouin, M.-M. Denariez-Roberge, P. Galarneau, J. Opt. Soc. Am. B 8 (1991) 578.
[9] A. Blouin, M.-M. Denariez-Roberge, IEEE J. Quantum Electron. 29 (1993) 227.
[10] V.V. Ivakhnik, V.I. Nikonov, Opt. Spektrosk. 75 (1993) 385, in Russian; Opt. Spectrosc. 75 (1993) 227.
[11] S.M. Karpuk, A.S. Rubanov, A.L. Tolstik, A.V. Chaley, Pis'ma Zh. Tekh. Fiz. 20 (1994) 2 4, in Russian; Sov. J. Technol Phys. Lett. 20 (1994) 475.
[12] S.M. Karpuk, A.S. Rubanov, A.L. Tolstik, Opt. Spektrosk. 80 (1996) 313, in Russian; Opt. Spectrosc. 80 (1996) 276.
[13] S.M. Karpuk, A.S. Rubanov, A.L. Tolstik, Kvant. Elektron. 24 (1997) 52, in Russian; Sov. J. Quantum Electron. 27 (1997) 49.
[14] R.H. Pantell, H.E. Puthoff, Fundamentals of Quantum Electronics, Wiley, New York, 1969.
[15] V.V. Kabanov, A.S. Rubanov, Dokl. Akad. Nauk BSSR 24 (1980) 34, in Russian.
[16] V.V. Kabanov, A.S. Rubanov, A.L. Tolstik, Kvant. Elektron. 15 (1988) 1681, in Russian; Sov. J. Quantum Electron. 18 (1988) 1047.
[17] A.V. Masalov, V.A. Petukhov, N.V. Timokhovich, L.B. Vodovatov, M.V. Gorbunkov, Kvant. Elektron. 18 (1991) 749, in Russian; Sov. J. Quantum Electron. 21 (1991) 680.
[18] S.M. Karpuk, A.S. Rubanov, A.L. Tolstik, A.V. Chaley, Proc. SPIE 2051 (1993) 974.
[19] C. Wu, J. Fan, Z. Wang, Proc. Int. Conf. on Lasers, Beijing – Shanghai, 1980, p. 231.
[20] S.M. Karpuk, O.G. Romanov, A.S. Rubanov, A.L. Tolstik, Bulletin of the Russian Academy of Sciences. Physics/ Supplement: Physics of Vibrations 60 (1996) 52.
[21] V.I. Prokhorenko, M.V. Melishchuk, E.A. Tikhonov, Ukr. Fiz. Zh. 30 (1985) 1480, in Russian.
[22] M.A. Vasil'eva, V.B. Gul'binas, V.I. Kabelka, A.V. Masalov, V.P. Syrus, Kvant. Elektron. 10 (1983) 415, in Russian; Sov. J. Quantum Electron. 13 (1983) 233.
[23] M.H. Garrett, H.J. Hoffman, J. Opt. Soc. Am. 73 (1983) 617.
[24] A. Tolstik, Proc. SPIE 3580 (1998) 73.